ACS Biomaterials SCIENCE & ENGINEERING
Cite This: ACS Biomater. Sci. Eng. 2018, 4, 4354−4366
Article
pubs.acs.org/journal/abseba

Differential Effects of Heparin and Hyaluronic Acid on Neural Patterning of Human Induced Pluripotent Stem Cells

Julie Bejoy,[†,∥] Zhe Wang,[‡,⊥] Brent Bijonowski,[†,∥] Mo Yang,[‡,⊥] Teng Ma,[†,∥] Qing-Xiang Sang,[‡,§,⊥] and Yan Li*[,†,§,∥]

[†]Department of Chemical and Biomedical Engineering, FAMU-FSU College of Engineering, Florida State University, Tallahassee, Florida, United States

[‡]Department of Chemistry and Biochemistry, Florida State University, Tallahassee, Florida, United States

[§]Institute of Molecular Biophysics, Florida State University, Tallahassee, Florida, United States

Supporting Information

ABSTRACT: A lack of well-established animal models that can efficiently represent human brain pathology has led to the development of human induced pluripotent stem cell (hiPSC)-derived brain tissues. Brain organoids have enhanced our ability to understand the developing human brain and brain disorders (e.g., Schizophrenia, microcephaly), but the organoids still do not accurately recapitulate the anatomical organization of the human brain. Therefore, it is important to evaluate and optimize induction and signaling factors in order to engineer the next generation of brain organoids. In this study, the impact of hyaluronic acid (HA), a major brain extracellular matrix (ECM) component that interacts with cells through ligand-binding receptors, on the patterning of brain organoids from hiPSCs was evaluated. To mediate HA-binding capacity of signaling molecules, heparin was added in addition to HA or conjugated to HA to form hydrogels (with two different moduli). The neural cortical spheroids derived from hiPSCs were treated with either HA or heparin plus HA (Hep-HA) and were analyzed for ECM impacts on neural patterning. The results indicate that Hep-HA has a caudalizing effect on hiPSC-derived neural spheroids, in particular for stiff Hep-HA hydrogels. Wnt and Hippo/Yes-associated protein (YAP) signaling was modulated (using Wnt inhibitor IWP4 or actin disruption agent Cytochalasin D respectively) to understand the underlying mechanism. IWP4 and cytochalasin D promote forebrain identity. The results from this study should enhance the understanding of influence of biomimetic ECM factors for brain organoid generation.

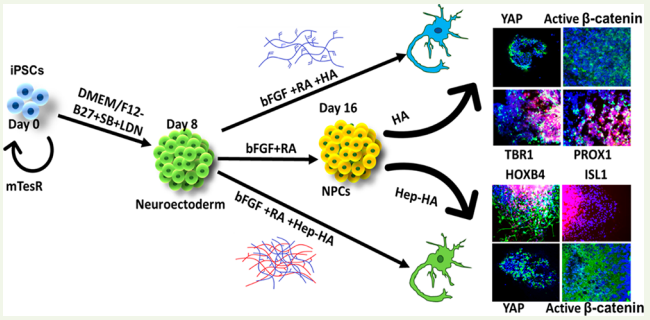

KEYWORDS: *induced pluripotent stem cells, heparin, hyaluronic acid, neural patterning, spheroids, hydrogels*

INTRODUCTION

Various types of brain spheroids or organoids have been derived from human induced pluripotent stem cells (hiPSCs) recently to study neurological diseases (e.g., microcephaly) and virus infection (e.g., ZIKV virus),[1−9] and for drug screening.[10] While some key features (such as cortical layer separation) make these spheroids or organoids attractive in modeling neurological diseases and brain development, full resemblance to the human brain is still not achieved, and the brain tissues are usually developmentally immature.[5,11] Therefore, the spatially compartmentalized microenvironments and the spatial-temporal regulation of the induction factor gradients become important in developing the next generation of brain organoids.[11,12]

During brain organoid formation, extracellular matrix (ECM) hydrogels,[11−15] such as Matrigel,[1] collagen gels,[16] and poly(ethylene glycol) (PEG) hydrogels,[17−19] can provide instructive extracellular signals for hiPSC self-assembly into aggregates and facilitate neural tissue development.[8] Matrigel is an undefined extract derived from mouse Engelbreth−Holm−Swarm tumors and composed of 60% laminin. PEG is similar to the ECM as far as its hydration properties, molecular weight, and organic nature. As a synthetic hydrogel, it is not chemically similar to sugar or proteins in the brain. A novel hydrogel, Amikagel (modified based on PEG), was reported for islet organoid formation and shown to enhance islet-specific marker expression.[20] A chemically defined hydrogel composed of hyaluronan and chitosan protonated with formic acid was recently reported for cerebral organoid generation from hPSCs.[21] Taken together, the importance of cell−matrix interactions during organoid formation was recognized recently.[11,22]

Hyaluronan, also called hyaluronic acid (HA), is a biodegradable polymer that is a part of brain ECM[23] and has

Received: September 19, 2018
Accepted: November 4, 2018
Published: November 4, 2018

DOI: 10.1021/acsbiomaterials.8b01142
ACS Biomater. Sci. Eng. 2018, 4, 4354−4366

been successfully used to improve transplantation survival rates of neural progenitor cells.[24−28] Due to its brain-mimetic and fully defined properties, HA is a strong hydrogel candidate for brain tissue engineering and transplantation.[27] Effects of HA on cells have been found to be mediated by the interaction of HA with several receptors including CD44, the receptor for hyaluronic-acid-mediated motility (RHAMM), and intercellular adhesion molecule 1 (ICAM1).[29] HA hydrogels also have tunable mechanical properties (e.g., elastic modulus) and can be grafted with other ECM proteins or functionalized with adhesive peptides (e.g., RGD) or growth-factor-binding factors (e.g., heparin).[30−34] Therefore, HA is suitable to be used in the culture system for brain organoid generation from hiPSCs.

Heparin, an analog of heparan sulfate proteoglycans (HSPG),[35,36] is a glycosaminoglycan with neurotrophic factor binding ability and may be a modulator for the Wnt pathway.[37] It was suggested that heparin plays a biphasic role in modulating Wnt signaling.[38] Heparin upregulates Wnt3a expression at an early induction stage (mesoderm) but inhibits Axin2, a downstream effector of Wnt, at a later stage. For ectoderm, heparin was reported to activate Wnt signaling through inducing glycogen synthase kinase-3β (GSK-3β) inhibition and β-catenin stabilization.[39] Similarly, the core protein of HSPGs is important for Wnt protein stabilization.[40] The aggregation of Wnt proteins in aqueous environments is prevented by direct interaction between proteoglycans and Wnt proteins.[40] Heparin also contributes to the accumulation of secreted Frizzled-related proteins (sFRPs), which act as a biphasic modulator of Wnt, either by direct stabilization or by stabilization of sulfated sFRPs.[41] While HA-based hydrogels functionalized with heparin have been evaluated for cell transplantation and growth factor release, their influence on the Wnt pathway, which can pattern neural tissue derived from hiPSCs along the rostral and caudal brain identity,[42,43] for brain organoid formation has not been well understood.

The objective of this study is to investigate the synergistic effects of heparin and hyaluronic acid on neural patterning of hiPSCs for applications in brain organoid engineering and disease modeling. Geltrex, a similar ECM mixture to Matrigel, and Gelatin (GA), a common type of ECM derived from collagens, were included for comparison. The regional identity markers were compared for Geltrex (in the control group), Gelatin, HA, and heparin-HA groups. Furthermore, the heparin-HA hydrogels were characterized for use on spheroid patterning. The heparin-HA group promotes caudal tissue identity possibly by activation of canonical Wnt signaling. Therefore, the effects of Wnt inhibitor IWP4 and the actin disruption agent Cytochalasin D were evaluated. This study should facilitate the rational design of defined hydrogels and the control of induction factor gradients for brain organoid generation with biomimetic physiology.

MATERIALS AND METHODS

Undifferentiated hiPSC Culture. Human iPSK3 cells were derived from human foreskin fibroblasts transfected with plasmid DNA encoding reprogramming factors OCT4, NANOG, SOX2, and LIN28 (kindly provided by Dr. Stephen Duncan, Medical College of Wisconsin).[44,45] Human iPSK3 cells were maintained in mTeSR serum-free medium (StemCell Technologies, Inc., Vancouver, Canada) on a growth factor reduced Geltrex-coated surface (Life Technologies).[46] The cells were passaged by Accutase every 5−6 days and seeded at 1×10^6 cells per well of a six-well plate in the presence of 10 μM Y27632 (Sigma) for the first 24 h.[43,46,47]

ECM Preparation. Gelatin solution was prepared by adding the gelatin B powder (Sigma-Aldrich) to sterile phosphate buffer saline (PBS) solution at 6−12 mg/mL. Hyaluronic acid sodium salt powder (HA; 200 kDa, Sigma-Aldrich) was dissolved in sterile PBS at 6−12 mg/mL. For heparin-HA conditions, the heparin (Sigma-Aldrich) was added to HA solution at 10 μg/mL. All the ECMs were added at day 17 or day 9 of cell culture on the plates coated with 1% geltrex. The resulting concentrations of ECMs were at 0.5 wt % (5 mg/mL) for GA, 0.5 wt % (5 mg/mL) for HA, and 10 μg/mL for heparin. For control conditions, no ECM was added. The cells were maintained in the ECM-containing media for 4−5 days and then harvested for staining or quantification.

Preparation of Heparin-HA Hydrogels through Photo-Cross-Linking. Heparin-HA hydrogels were prepared using a modified procedure.[48] Briefly, to synthesize methacrylated hyaluronic acid (MA-HA), 1% (w/v) HA solution was reacted with a 3.5-fold molar excess amount of methacrylic anhydride (Sigma) for 15 h in the dark at 4 °C while maintaining pH at 8−11 using 1 N NaOH. The final product was collected by precipitating the solution in a 5-fold volume of ethanol twice and purified by dialysis against deionized water (DIW) using a dialysis membrane (3.5 kDa Mw cutoff, Thermofisher) to remove unreacted reagents. Purified MA-HA was filtered, lyophilized, and stored at −20 °C until further use. ^{1}H NMR spectroscopy (a Bruker Avance III 400 MHz spectrometer) was used to analyze the degree of methacrylation (Supporting Information Figure S1).

To synthesize thiolated heparin (Hep-SH), 10 mg/mL of heparin sodium salt was reacted with 1.75-fold 1-ethyl-3-[3-dimethylamino]-propyl]carbodiimide (EDC), 1.75-fold 1-hydroxy-benzotriazole hydrate (HOBt), and 2-fold cysteamine (all from Sigma) for 5 h with stirring at room temperature while maintaining the pH at 6.8 with 0.1 M NaOH and/or HCl solution.[49] The reaction solution was exhaustively dialyzed using a dialysis membrane (3.5 kDa Mw cutoff) to remove unreacted reagents. Then, a 10-fold molar excess of dithiotreitol (DTT, ThermoFisher) was added to the solution and reacted for 3 h at pH 7.5 to free thiol groups. After that, pH was adjusted to 3.5 by adding 1.0 N HCl to stop the reaction. The acidified solution was dialyzed against a dilute HCl at pH 3.5 buffer containing 100 mM NaCl, followed by dialysis against dilute HCl at pH 3.5. Hep-SH was further purified by running a PD-10 desalting column (Sigma) and lyophilized. The conversion from COOH to SH was tested by Ellman assay at 412 nm (Supporting Information Figure S2). Purified Hep-SH was filtered, lyophilized, and stored at −20 °C until further use.

Hep-SH and HA-MA were dissolved in PBS at a 1:1 molar ratio of thiol/acrylate. The solution of 0.01% (w/v) Eosin Y was added to the polymer precursor solution as a photo initiator, and the pH of the reaction mixture was adjusted to 7.8. The precursor mixture (2 wt %, 70 μL) was then transferred to a clean glass slide and covered with a clean coverslip with 300 μm thickness and photopolymerized under 525 nm green LED light exposure for 15 min. The 4 wt % precursor solution was also used to make a Hep-HA hydrogel with a higher modulus. Mechanical properties for Hep-HA hydrogels were measured with a Discovery Hybrid Rheometer (TA Instruments, USA) using a constant strain of 30% with a frequency sweep from 0.1 to 10 rad/s at 37 °C. The fully swollen state hydrogels were obtained by incubating them in PBS for 2 days (pH 7.4, 37 °C). The swelling ratio of hydrogels was analyzed by the weight ratio of fully swollen state (Ws) to dry (lyophilized) state (Wd) as Ws/Wd.

Effects of Different ECMs on Pluripotency and Three-Germ Layer Markers. To evaluate the impact of these ECMs on the differentiation potential, the cells were treated with the ECMs for 10 days in mTeSR culture medium and low attachment 24-well plates. At day 10, the cells were replated onto tissue-culture-treated plates and used for further imaging and quantitative analysis. The pluripotency of the cells was evaluated for Oct4 and Nanog expression. The differentiation potential was evaluated using three-germ-layer markers: β-tubulin III (ectoderm), Nkx 2.5 (mesoderm), and FOXA2 (endoderm).

DOI: 10.1021/acsbiomaterials.8b01142
ACS Biomater. Sci. Eng. 2018, 4, 4354−4366

Cortical Spheroid Differentiation of hiPSCs. Human iPSK3 cells were seeded into Ultra-Low Attachment (ULA) 24-well plates (Corning Incorporated, Corning, NY) at 3×10^5 cells/well in differentiation medium composed of Dulbecco's Modified Eagle Medium/Nutrient Mixture F-12 (DMEM/F-12) plus 2% B27 serum-free supplement (Life Technologies). Y27632 (10 μM) was added during the seeding and removed after 24 h. At day 1, the cells formed spheroids and were treated with dual SMAD signaling inhibitors 10 μM SB431542 (Sigma) and 100 nM LDN193189 (Sigma).[50,51] After 8 days, the cells were treated with fibroblast growth factor (FGF)-2 (10 ng/mL, Life Technologies, also known as basic FGF, i.e., bFGF) and retinoic acid (RA; 5 μM, Sigma) until day 16. At day 17, the spheroids were replated onto geltrex-coated tissue culture plates together with different ECMs (Table 1). For some experiments, different ECMs were added to the culture at day 8. For hydrogel experiments, a total of 20 uL per well of sterilized Hep-HA hydrogel precursors were transferred into a 96-well plate and photo-cross-linked for 15 min before spheroids were replated. The replated spheroids within hydrogels were stained for immunocytochemistry assays, dissociated (by trypsin/EDTA) for flow cytometry assay, and isolated for mRNA analysis.

Table 1. Summary of Experimental Conditions

Figures	ECM components	differentiation conditions
Figure 1	add heparin and HA in solution	three-germ layer differentiation
Figure 2	add heparin and HA in solution	treated during day16−21
Figure 3	add heparin and HA in solution	treated during day 8−21 or day16−21
Figure 4	add heparin and HA in solution	treated during day16−21
Figure 5	add heparin and HA in solution	treated during day16−21
Figure 6	add heparin and HA in solution	treated during day16−21
Figure 7	photo-cross-linked Hep-HA hydrogels	not applicable
Figure 8	photo-cross-linked Hep-HA hydrogels	treated during day16−21

Immunocytochemistry. Briefly, the samples were fixed with 4% paraformaldehyde (PFA) and permeabilized with 0.2−0.5% Triton X-100. The samples were then blocked for 30 min and incubated with various mouse or rabbit primary antibodies (Supporting Information Table S1) for 4 h. After washing, the cells were incubated with the corresponding secondary antibody: Alexa Fluor 488 goat anti-Mouse IgG_1, Alexa Fluor 594 goat anti-Rabbit IgG, or 594 donkey antigoat IgG (Life Technologies) for 1 h. The samples were counterstained with Hoechst 33342 and visualized using a fluorescent microscope (Olympus IX70, Melville, NY) or a confocal microscope (Zeiss LSM 880). The images from five independent fields (800−1000 cells) were analyzed using ImageJ software. The intensity was calculated based on the area of the marker of interest normalized to the nuclei, indicating the relative expression among different conditions.[50,52] For the 5-bromo-2′-deoxyuridine (BrdU) assay, the cells were incubated in a medium containing 10 μM BrdU (Sigma) for 4 h. The cells were then fixed with 70% cold ethanol, followed by a denaturation step using 2 N HCl/0.5% Triton X-100 for 30 min in the dark. The samples were reduced with 1 mg/mL sodium borohydride for 5 min and incubated with mouse anti-BrdU (1:100, Life Technologies) in a blocking buffer (0.5% Tween 20/1% bovine serum albumin in PBS), followed by Alexa Fluor 488 goat anti-Mouse IgG_1 (Molecular Probes). The cells were counterstained with Hoechst 33342 and analyzed using a fluorescent microscope and the ImageJ software.

Flow Cytometry. To quantify the levels of various neural marker expressions, the cells were harvested by trypsinization and analyzed by flow cytometry.[53] Briefly, 1×10^6 cells per sample were fixed with 4% PFA and washed with staining buffer (2% fetal bovine serum in PBS). The cells were permeabilized with 100% cold methanol, blocked, and then incubated with various primary antibodies (Supporting Information Table S1; for 1−4 h) followed by the corresponding secondary antibody (for 30−60 min) Alexa Fluor 488 goat anti-Mouse IgG_1 or Alexa Fluor 594 Goat Antirabbit or Donkey Anti-Goat IgG. The cells were acquired with BD FACSCanto II flow cytometer (Becton Dickinson) and analyzed against isotype controls using FlowJo software.

Western Blotting. Cells were pelleted, washed with ice cold PBS, and lysed in a hypotonic buffer containing 20 mM HEPES (pH 7.4), 10 mM KCl, 2 mM $MgCl_2$, 1 mM EDTA, 1 mM EGTA, and 1% fresh DTT. Lysates were examined under a microscope to ensure only nuclei were visible. The lysate was centrifuged at 800g for 5 min to separate nuclei and cytoplasmic fractions. NP-40 buffer was added to lyse and resuspend the nuclei pellet. Protein concentration of the lysed samples was determined via Bradford assay. Protein lysate concentration was normalized, and 20 μg of each sample was resolved on a 10% running/4% stacking SDS-PAGE gel for 20 min at 100 V and then at 200 V until the end. Proteins were then transferred onto nitrocellulose membranes at 100 V for 1 h. Then the blots were blocked with 3% milk TBS-Tween 20 (TBST) solution for 30 min. After blocking, the blots were probed with 0.05 μg/mL active β-catenin, 1:10,000 β-tubulin (endogenous cytoplasmic control), or lamin B1 (endogenous nuclear control) antibody in 3% milk/TBST overnight at 4 °C. After washing with TBST, each blot was incubated with 1:10 000 antirabbit or antimouse Li-Cor (Linclon, NE) infrared secondary antibody for 1 h. Finally, blots were washed with TBST, and imaged on a Li-Cor Odyssey imager.

Biochemical Assays. The cells were evaluated for viability using a Live/Dead staining kit (Molecular Probes). After 72 h, the cells were incubated in DMEM-F12 containing 1 μM calcein-AM (green) and 2 μM ethidium homodimer I (red) for 30 min. The samples were imaged under a fluorescent microscope (Olympus IX70, Melville, NY). Using ImageJ software, the viability was analyzed and calculated as the percentage of green intensity over total intensity (including both green cells and red cells). For MTT assay, the replated neural cells were incubated with 5 mg/mL 3-(4,5-dimethylthiazol-2-yl)-2,5-diphenyltetrazolium bromide (MTT, Sigma) solution. The absorbance was measured at 500 nm using a microplate reader (Bio-Rad iMark).

Effects of IWP4 and Cyto D. To evaluate the Wnt signaling impact, the cells at day 8 were treated with Wnt inhibitor IWP4 (5 μM, Stemgent) together with different ECMs. The cells grown in medium containing IWP4 alone were kept as the control. The medium was replaced every 2 days, and the cells were replated at day 16. The replated cells were analyzed for immunocytochemistry or flow cytometry at day 20. The neural cells were immunostained for hindbrain markers HOXB4, ISL1, and forebrain markers TBR1 and PROX1. To evaluate the impact of Hippo/YAP signaling, the stress fiber disruptor Cytochalasin D (2 μM, Sigma) was added to the replated cells together with the ECMs at day 16. The cells were then analyzed for immunocytochemistry or flow cytometry at day 20. Hindbrain marker HOXB4 and forebrain ventral marker PROX1 were analyzed.

Reverse Transcription-Polymerase Chain Reaction (RT-PCR) Analysis. Total RNA was isolated from neural cell samples using the RNeasy Mini Kit (Qiagen, Valencia, CA) according to the manufacturer's protocol followed by treatment with the DNA-Free RNA Kit (Zymo, Irvine, CA). Reverse transcription was carried out using 2 μg of total RNA, anchored oligo-dT primers (Operon, Huntsville, AL), and Superscript III (Invitrogen, Carlsbad, CA; according to the protocol of the manufacturer). Primers specific for target genes (Supporting Information Table S2) were designed using the software Oligo Explorer 1.2 (Genelink, Hawthorne, NY). The gene β-actin was used as an endogenous control for normalization of expression levels. Real-time RT-PCR reactions were performed on an ABI7500 instrument (Applied Biosystems, Foster City, CA), using SYBR1 Green PCR Master Mix (Applied Biosystems). The amplification reactions were performed as follows: 2 min at 50 °C; 10 min at 95 °C; and 40 cycles of 95 °C for 15 s, 55 °C for 30 s, and 68 °C for 30 s. Fold variation in gene expression was quantified by means of the comparative C_t method: $2^{-(C_{t\text{-treatment}} - C_{t\text{-control}})}$, which is based on the comparison of expression of the target gene (normalized to the endogenous control β-actin) among different conditions.

DOI: 10.1021/acsbiomaterials.8b01142
ACS Biomater. Sci. Eng. 2018, 4, 4354−4366

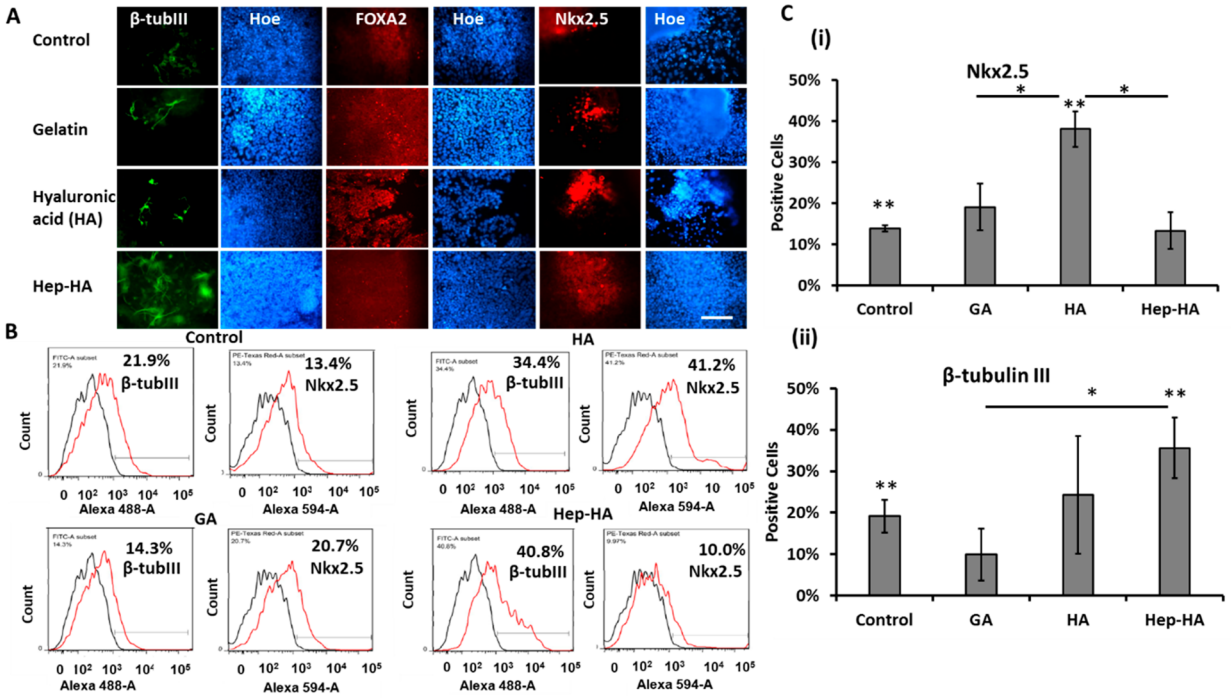

Figure 1. Expression of three-germ layer differentiation markers of ECM-treated hiPSCs. The cells treated with ECMs were analyzed for three-germ layer markers. (A) Fluorescent images of β-tubulin III (ectoderm), Nkx2.5 (mesoderm), and FOXA2 (endoderm). Scale bar: 100 μm. (B) Representative flow cytometry histograms of β-tubulin III or Nkx2.5. Black line, negative control; red line, marker of interest. (C) Quantification of β-tubulin III or Nkx2.5 by flow cytometry (n = 3). (One-way ANOVA, F-value = 17.22 and P-value = 0.01 for Nkx2.5; F-value = 2.97 and P-value = 0.16 for β-tubulin III.) Control indicates Geltrex condition. * and ** indicate $p < 0.05$ between the marked conditions.

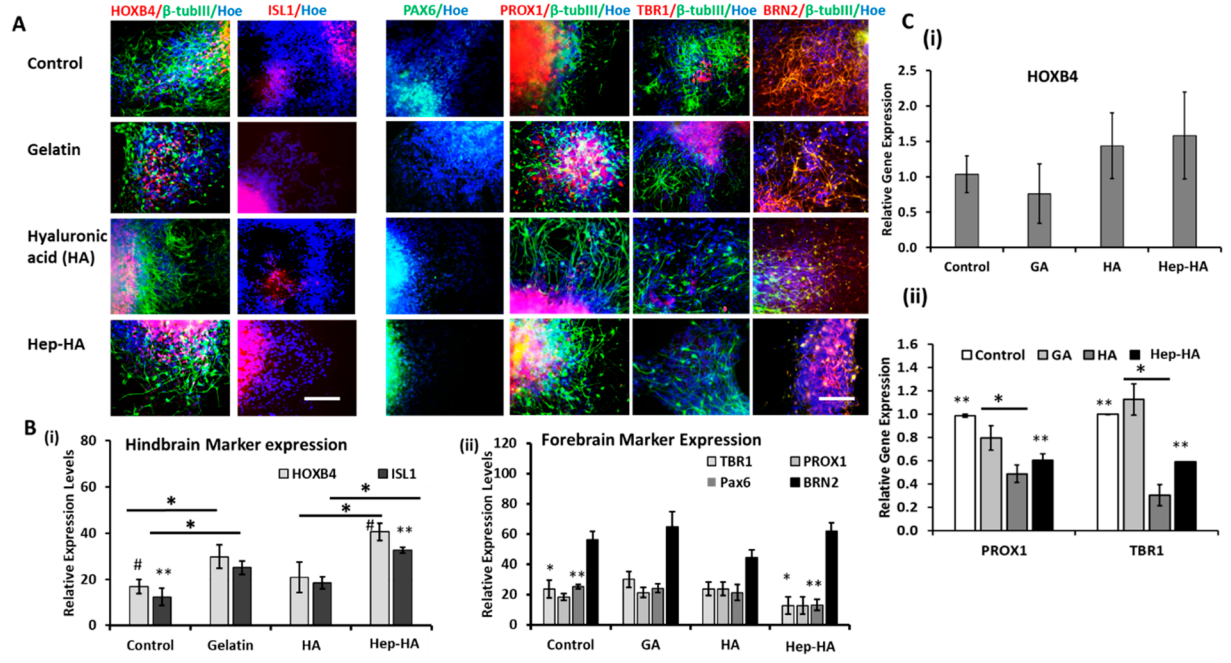

Figure 2. Effect of ECMs on neural tissue patterning of hiPSCs. The cells treated with ECMs at day 16 were analyzed for forebrain and hindbrain markers. (A) Fluorescent images of forebrain markers (PROX1, TBR1, BRN2, and PAX6) and hindbrain markers (HOXB4, ISL1) at day 20. Scale bar: 100 μm. (B) Quantification of expression using the ImageJ software (n = 3–5). (i) Hindbrain markers (HOXB4, ISL1; one-way ANOVA, F-value = 10.49, P-value < 0.001). (ii) Forebrain markers (PROX1, TBR1, BRN2, and PAX6; one-way ANOVA, F-value = 22.29, P-value < 0.001). (C) RT-PCR analysis of (i) HOXB4 and (ii) PROX1 and TBR1 gene expression (n = 3; one-way ANOVA, PROX1: F-value = 9.568, P-value = 0.03; TBR1: F-value = 21.22, P-value = 0.01). Control indicates Geltrex condition. *, **, and # indicate $p < 0.05$ between the marked conditions.

Statistical Analysis. Each experiment was carried out at least three times. The representative experiments were presented, and the results were expressed as mean ± standard deviation. To assess the statistical significance, one-way ANOVA followed by Fisher's LSD post hoc tests or two-way ANOVA followed by Tukey's post hoc tests

DOI: 10.1021/acsbiomaterials.8b01142
ACS Biomater. Sci. Eng. 2018, 4, 4354–4366

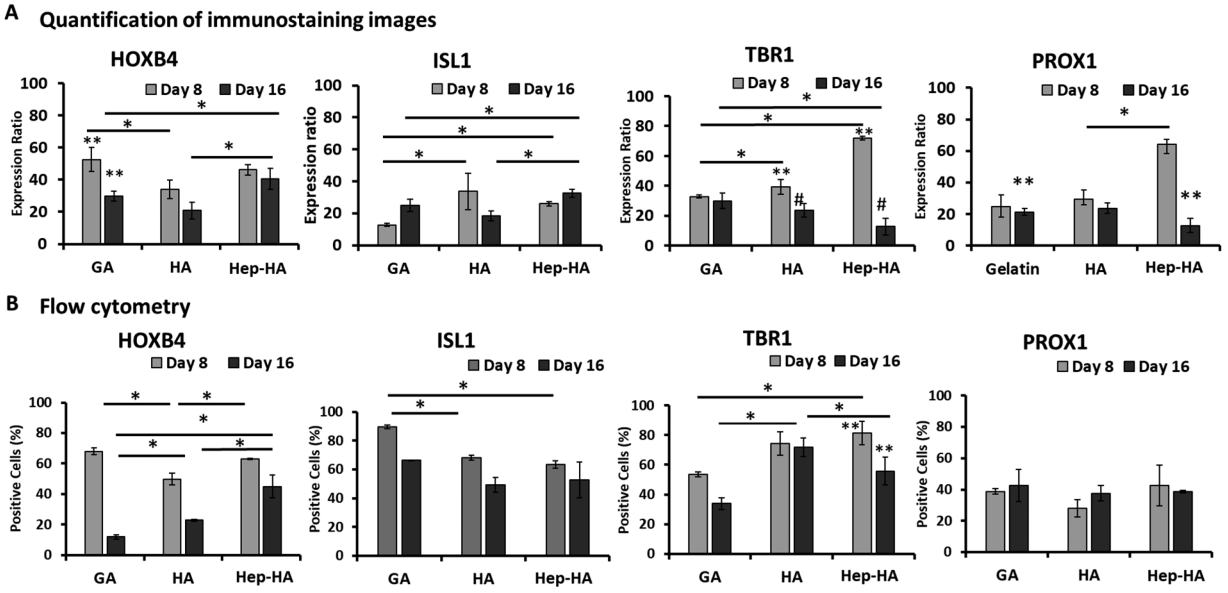

Figure 3. Stage-dependent impact of ECMs on neural tissue patterning of hiPSCs. The cells treated with ECMs at both day 8 and day 16 were compared for forebrain and hindbrain marker expression. (A) Quantification of marker expression using the ImageJ software for immunostaining images (n = 3). (B) Flow cytometry analysis of forebrain markers (TBR1, PROX1) and hindbrain markers (HOXB4, ISL1) at day 21 (n = 3). *, **, and # indicate $p < 0.05$ (two-way ANOVA, see Supporting Information Table S3).

were performed. A p value < 0.05 was considered statistically significant.

RESULTS

Heparin-Hyaluronic Acid Promotes Ectoderm Differentiation. Stem cells' fate decisions are influenced by their interactions with the local microenvironment. Thus, hiPSCs were treated with ECMs in mTeSR medium for 10 days to examine their spontaneous differentiation. The cells replated at day 10 were immunostained for pluripotency markers Oct-4 and Nanog and three germ layer markers including β-tubulin III (ectoderm), Nkx2.5 (mesoderm), and FOXA2 (endoderm; Figure 1A, Supporting Information Figure S3). The numbers of Oct-4$^+$ and Nanog$^+$ cells decreased for the three ECM groups compared to the control (the Geltrex), indicating spontaneous differentiation (Supporting Information Figure S3). For three-germ layer markers quantified by flow cytometry, more cells in the HA-treated group expressed mesodermal marker Nkx2.5 (38.2 ± 4.3% vs 14.0 ± 0.8%) compared to the control (Figure 1B,C). The cells with heparin plus HA treatment expressed a higher level of ectodermal marker β-tubulin III (35.6 ± 7.4% vs 19.2 ± 3.9%) compared to the control, suggesting that Hep-HA favors neural differentiation (Figure 1B,C).

Effect of Hep-HA Condition on Neural Tissue Patterning. The influence of Hep-HA on neural patterning of hiPSC-derived cortical spheroids was then evaluated. The hiPSCs were induced toward cortical neural lineage with LDN/SB treatment (dual SMAD inhibition) followed by FGF-2/RA treatment for 16 days (Supporting Information Figure S4).[50] The neural progenitor cell (NPC) spheroids were replated and treated with three types of ECMs at day 1 after replating. At day 16 + 5, the cells were analyzed for cell viability and patterning effect. Hep-HA group had higher MTT activity and viability compared to the control, while the HA group had lower viability than the control (Supporting Information Figure S5). Neural cells for the three groups displayed 15−33% of Nestin (early neural progenitors) and 78−88% of β-tubulin III (neurons) expression (Supporting Information Figure S6). The replated outgrowth was then immunostained for hindbrain markers HOXB4 (hindbrain/spinal cord) and ISL1 (a marker for motor neurons) and forebrain markers TBR1 (a deep cortica layer VI marker), PROX1 (a marker for forebrain hippocampus neural progenitos), BRN2 (a superficial cortical layer II−IV marker), and PAX6 (a forebrain marker). GA treatment resulted in similar expression for the forebrain markers compared to the control (Figure 2A,B). The expression of hindbrain markers HOXB4 and ISL1 was higher for the Hep-HA group compared to the control (Figure 2B). Meanwhile, Hep-HA reduced the expression of forebrain markers TBR1, PROX1, and PAX6 (Figure 2A,B). RT-PCR analysis showed lower TBR1 and PROX1 expression for the HA and Hep-HA groups compared to the control (Figure 2C). While higher HOXB4 expression was observed, the difference was not statistically significant.

The cells were also stained for inhibitory and excitatory neurotransmitter markers glutamate and GABA. Abundant expression of glutamate and GABA were observed for all groups (Supporting Information Figure S7). The results indicate that Hep-HA may promote the expression of hindbrain/spinal cord neurons and reduce the expression of forebrain neurons.

Stage-Dependent Impact of ECMs on Neural Tissue Patterning of hiPSCs. To understand the stage-dependent impact of the Hep-HA on the neural patterning, the cells were treated with different ECMs at day 8 in comparison to day 16. Immunostaining and flow cytometry analysis were performed to evaluate the expression of various markers. The Hep-HA treatment at day 16 had higher HOXB4 than the GA and HA groups, but the Hep-HA treatment at day 8 had similar HOXB4 to the GA group, only higher than the HA group (Figure 3A,B). The Hep-HA treatment had higher ISL1 than the GA group based on immunostaining, but not flow cytometry (Figure 3A,B). For forebrain markers, the Hep-

DOI: 10.1021/acsbiomaterials.8b01142
ACS Biomater. Sci. Eng. 2018, 4, 4354−4366

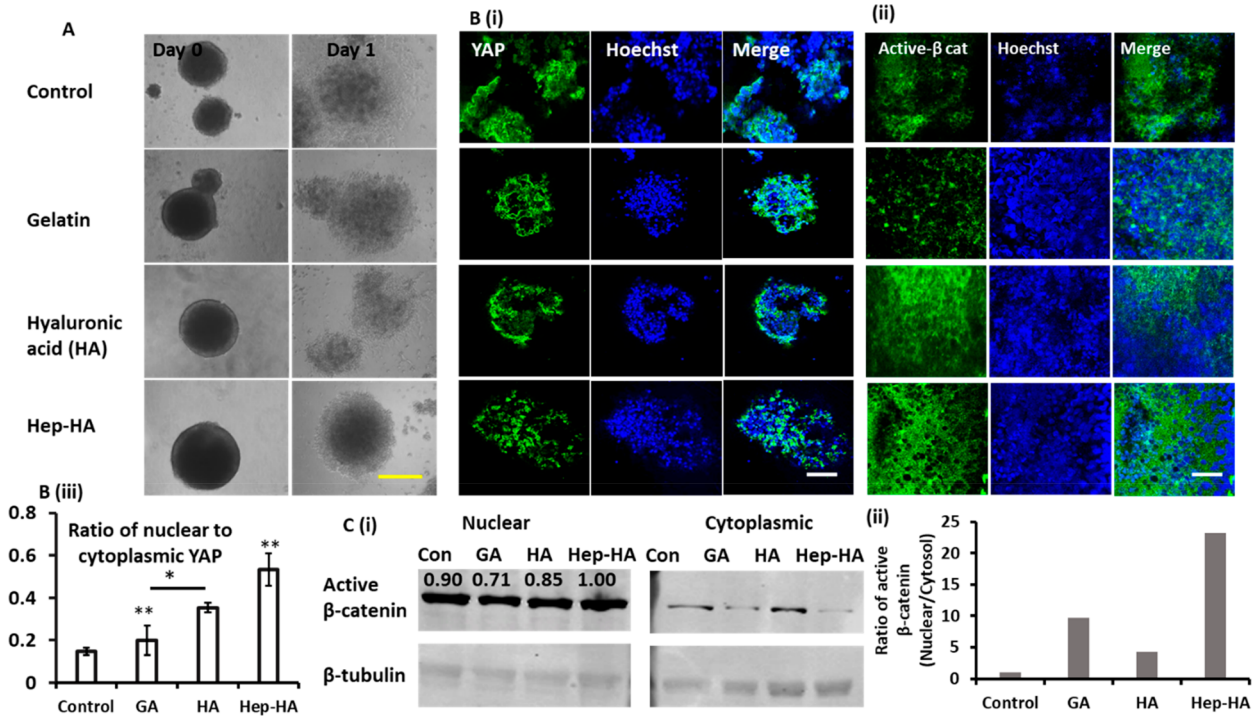

Figure 4. Effect of ECMs on YAP and active β-catenin expression. The cells treated with ECMs at day 16 were analyzed for YAP and active β-catenin expression (A) Phase contrast images of day 16 NPC aggregates replated at day 0 and day 1. Scale bar: 400 μm. (B) Confocal fluorescent images of (i) YAP and (ii) active β-catenin (active β-cat) at day 20. Scale bar: 50 μm. The negative circles of active β-catenin in the Hep-HA group did not colocalize with any blue nuclei, indicating that they were not associated with cells. (iii) Quantification of YAP expression (nuclear to cytoplasmic ratio; one-way ANOVA, F-value = 10.46, and P-value = 0.02). * and ** indicate $p < 0.05$. (C, i) Western blot bands of active β-catenin in nuclear and cytoplasmic proteins. The numbers above the bands showed the density quantification through image analysis. β-tubulin is endogenous cytoplasmic control. (ii) Quantification and normalization of active β-catenin expression (nuclear to cytoplasmic ratio). Control indicates Geltrex condition.

HA group had reduced TBR1 and PROX1 expression compared to the GA and HA groups based on immunostaining (Figure 3A). On the basis of flow cytometry, the Hep-HA group had reduced TBR1 compared to the HA group, but not the GA group. Variations exist for immunostaining image analysis and flow cytometry analysis, and flow cytometry analysis showed no significant difference among different groups for PROX1. Taken together, the caudalization effect of Hep-HA was mainly observed for day 16 conditions rather than day 8 conditions. As the differentiation protocol induces neural cells of forebrain identity by default, the results indicate that the Hep-HA may promote hindbrain marker expression at a later stage of neural development.

Neural Cell Spreading, Stress Fiber Formation, and YAP Localization. The neural spheroids grown with different ECMs were evaluated for spheroid spreading and stress fiber formation. The cell spreading for the GA group was comparable to the control cells (Figure 4), while the cells in the HA group showed less adhesion compared to the GA group. The addition of heparin to the HA group improved cell adhesion and spreading (Figure 4A). In addition, the cells grown with GA and Hep-HA developed large actin assemblies compared to the HA group (Supporting Information Figure S8A). BrdU staining showed that more positive cells were found for the control and GA groups (e.g., 58.9 ± 11.4% and 46.7 ± 10.0% respectively), but fewer $BrdU^+$ cells for the HA and Hep-HA groups (e.g., 26.3 ± 12.4% and 37.4 ± 6.7%, respectively; Supporting Information Figure S8B).

The cell morphological changes involve the relocalization of transcriptional regulatory factors YAP/TAZ. For the spheroids, the YAP expression on GA was more cytoplasmic (Figure 4Bi,Biii and Supporting Information Figure S9). The HA-treated neural cells expressed more nuclear YAP compared to the GA-treated cells, which might be due to HA-mediated attenuation of Hippo signaling by CD44 receptor expression.[54] High expression of nuclear YAP was observed for the Hep-HA group, suggesting that heparin may affect YAP localization (Figure 4Bi and Supporting Information Figure S9). Previous studies have shown that there exists a crosstalk between Wnt/β-catenin and YAP signaling.[43,55] So the expression of active β-catenin was evaluated in our study (Figure 4Bii,C, and Supporting Information Figure S10). Neural cells grown with GA express less active β-catenin. In particular, the Hep-HA group has the highest ratio of nuclear to cytoplasmic active β-catenin and nuclear active β-catenin expression. Therefore, the Hep-HA group may promote the activation of canonical Wnt signaling.

Impacts of Signaling Inhibition Molecules on Neural Patterning Effect of ECMs. In order to further understand the impact of different ECMs on neural patterning, the neural cells with ECMs were treated with Wnt inhibitor IWP4 (Figure 5 and Supporting Information Figure S11). Through quantification by flow cytometry, the results showed that GA +IWP4 treatment reduced ISL1 and PROX1 expression, while IWP4 treatment reduced ISL1 and increased TBR1 expression for the HA group. The cells treated with Hep-HA and IWP4 had reduction in HOXB4 and increased TBR1 expression.

DOI: 10.1021/acsbiomaterials.8b01142
ACS Biomater. Sci. Eng. 2018, 4, 4354−4366

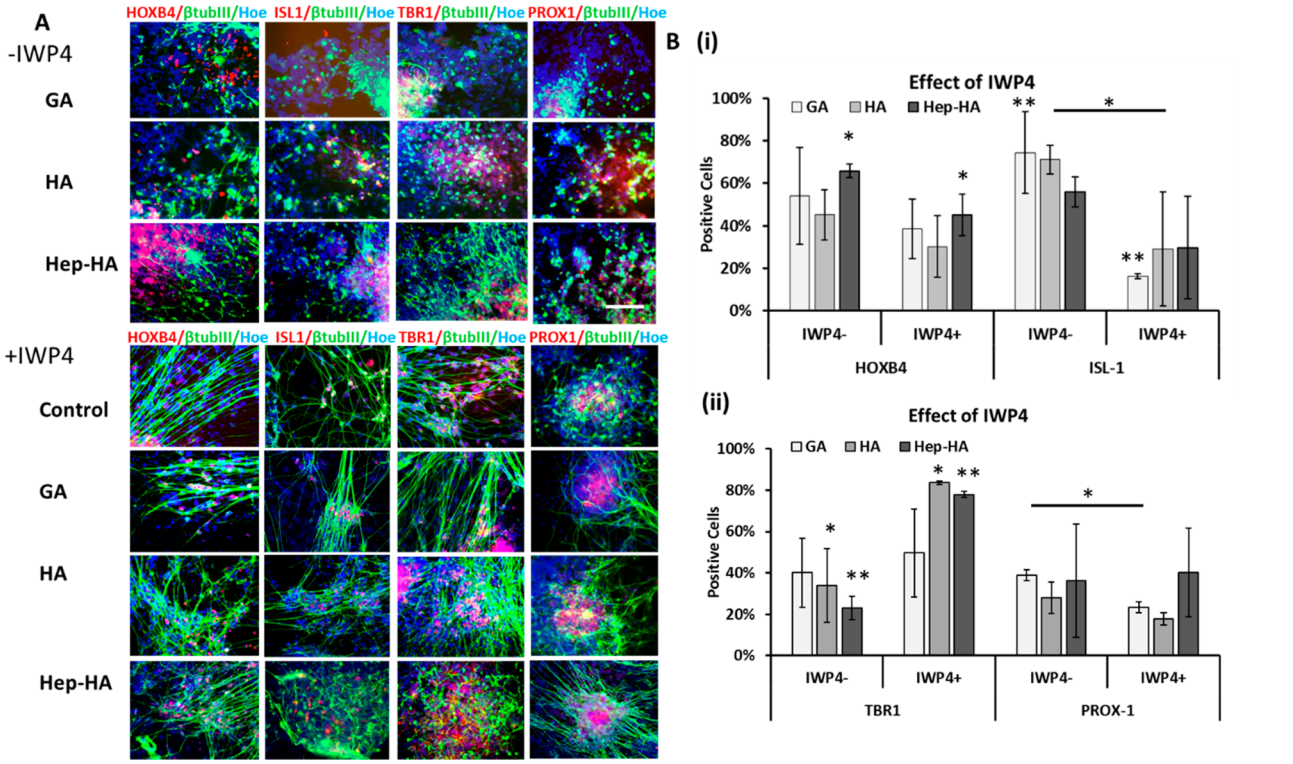

Figure 5. Effects of Wnt Inhibition on neural patterning of ECM treated-hiPSCs. The cells treated with ECMs and ±Wnt inhibitor IWP4 were analyzed for forebrain and hindbrain markers. (A) Fluorescent images of forebrain markers (PROX1, TBR1) and hindbrain markers (HOXB4, ISL1) at day 20 with ± IWP4. Scale bar: 100 μm. (B) Quantification of hindbrain (i) and forebrain (ii) marker expression at day 20 with ± IWP4 by flow cytometry (n = 3). Control indicates Geltrex conditions. * and ** indicate $p < 0.05$ (two-way ANOVA, see Supporting Information Table S3).

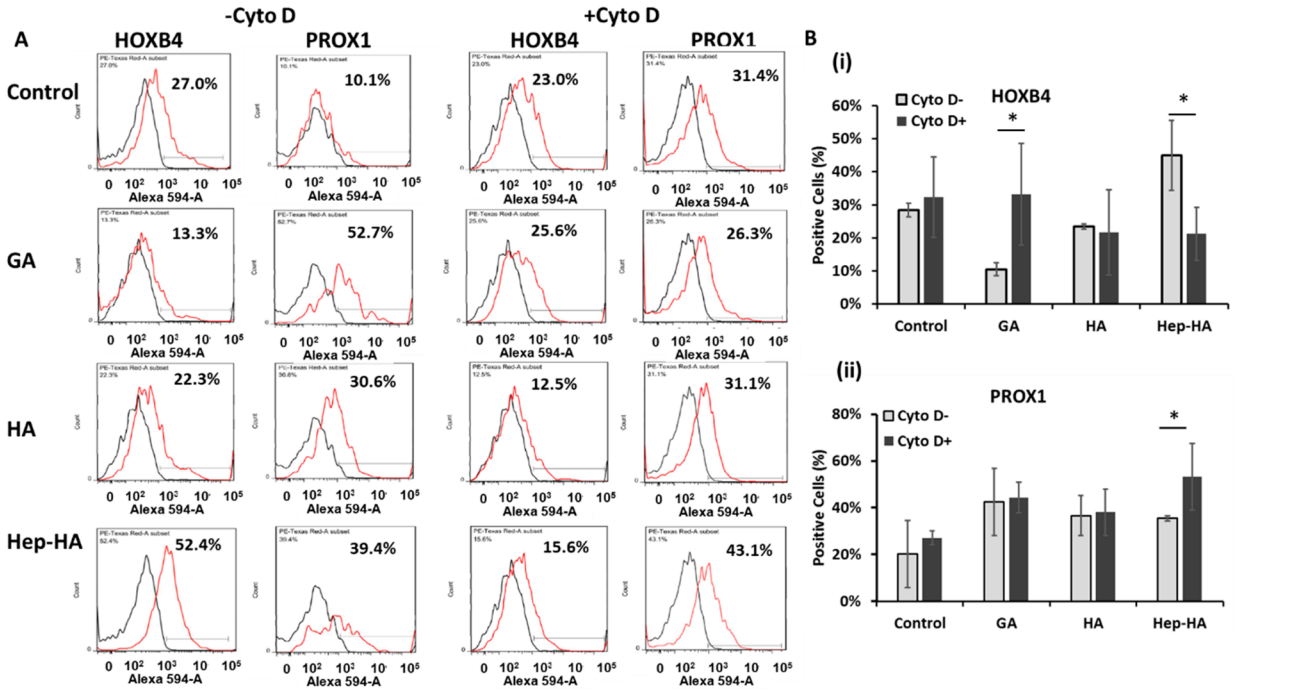

Figure 6. Effects of cytochalasin D treatment on neural patterning of ECM treated-hiPSCs. The cells treated with ECMs and ± cyto D at day 16 were analyzed for forebrain and hindbrain markers. (A) Representative flow cytometry histograms of forebrain marker (PROX1) and hindbrain marker (HOXB4) at day 20 under ± cyto D. Black line, negative control; red line, marker of interest. (B) Expression of (i) hindbrain marker HOXB4 and (ii) forebrain marker PROX1 at day 21 under ±cyto D quantified by flow cytometry (n = 3). Control indicates Geltrex conditions. * indicates $p < 0.05$ (two-way ANOVA, see Supporting Information Table S3).

DOI: 10.1021/acsbiomaterials.8b01142
ACS Biomater. Sci. Eng. 2018, 4, 4354−4366

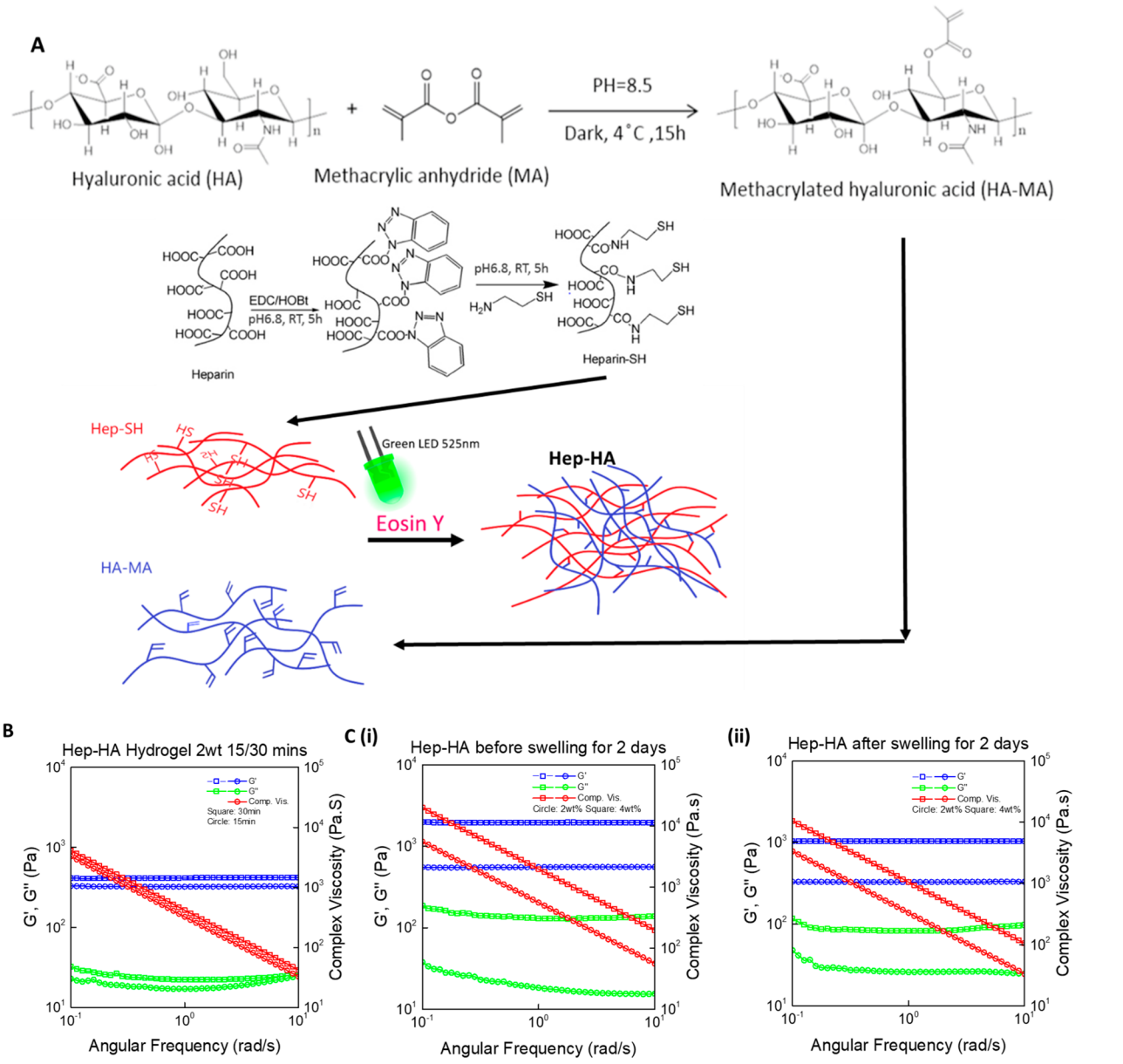

Figure 7. Fabrication and characterization of Hep-HA hydrogels. (A) Mechanism of methylation of HA (MA-HA), thiolation of heparin (Hep-SH), and the photo-cross-linking of MA-HA and Hep-SH. (B) Storage modulus of hydrogels under different lighting times, before and after swelling for 2 days, measured by a rheometer with a frequency sweep from 0.1 to 10 rad/s. (C) Storage modulus and swelling ratio of two types of hydrogels (2 and 4 wt %; n = 3).

These results indicate that cells with Hep-HA may exhibit elevated Wnt signaling.

Next, the impact of Hippo/YAP signaling was evaluated via cytochalasin D treatment (induces cytoplasmic YAP and inhibits Wnt signaling). The cells were examined for HOXB4 and PROX1 expression using flow cytometry analysis (Figure 6). The cyto D treatment increased the rostral brain marker PROX1 expression and decreased the expression of caudal marker HOXB4 for the Hep-HA group. These results suggest the crosstalks of a YAP-mediated patterning effect with canonical Wnt signaling.

Preparation and Characterization of Hep-HA Hydrogels and Effects of Modulus. Storage moduli of the stiff (4 wt %) and soft (2 wt %) hydrogels before and after swelling were measured to analyze mechanical properties of hydrogels. The light exposure times of 15, 30, and 45 min were examined. With 15 min-lighting, hydrogels reached an equilibrium state for cross-linking. However, when lighting for 45 min (data not shown), the storage modulus decreased possibly due to thermal degradation. The stiff hydrogels exhibited higher storage moduli and lower swelling ratios, indicating a tighter polymer network and higher cross-linking density than the soft hydrogels (Figure 7). After soaking in PBS for 2 days, the storage modulus of 2 and 4 wt % Hep-HA decreased from 573 ± 46 Pa to 333 ± 60 Pa and from 1762 ± 197 Pa to 1176 ± 137 Pa, respectively (Table 2). A lower swelling ratio was observed for 4 wt % Hep-HA as 29.4 ± 3.2 than 47.9 ± 7.3 for 2 wt % Hep-HA hydrogel.

Cortical spheroids were encapsulated within Hep-HA hydrogels of two different moduli (2 and 4 wt %; Figure 8A). On the basis of the expression of F-actin, the 4 wt % hydrogel promoted the stretching of F-actin compared to the 2

DOI: 10.1021/acsbiomaterials.8b01142
ACS Biomater. Sci. Eng. 2018, 4, 4354−4366

Table 2. Swell Ratio of Different Hep-HA Hydrogels

sample	soft Hep-HA	stiff Hep-HA
polymer concentration	2 wt %	4 wt %
before swelling storage modulus (G' = Pa)	573 ± 46[a]	1762 ± 197[a]
after swelling storage modulus (G' = Pa)	333 ± 60[a]	1176 ± 137[a]
swelling ratio (Ws/Wd)	47.9 ± 7.3	29.4 ± 3.2

[a] $p < 0.05$ between soft and stiff Hep-HA hydrogels.

wt % hydrogel (Figure 8B). The YAP localization showed more nuclear YAP for cells grown in the higher modulus hydrogel compared to the lower modulus (Figure 8B). Flow cytometry analysis showed that the cells within hydrogels with a higher modulus expressed the higher level of hindbrain marker HOXB4 (24.4 ± 0.9%) compared to the hydrogels with a lower modulus (14.4 ± 4.4%; Figure 8B,C). In the meanwhile, the expression of forebrain marker TBR1 by the cells in the lower modulus hydrogels was elevated (35.4 ± 3.5%) compared to the hydrogels with a higher modulus (17.0 ± 3.0%; Figure 8C). The cells also expressed another cortical marker BRN2 and hippocampal marker PROX1 (Supporting Information Figure S12). To further confirm the results, the cells treated with soluble Hep-HA and the Hep-HA hydrogels were analyzed for HOXB4, PROX1, and TBR1 gene expression using RT-PCR (Figure 8D). HOXB4 gene expression was higher for 4 wt % hydrogel than 2 wt % hydrogel, while PROX1 gene expression was lower for 4 wt % than 2 wt % hydrogels. No significant difference was found for TBR1 between 2% and 4% hydrogels. It was noted that compared to soluble Hep-HA conditions, in which the cells grew on a tissue culture-treated surface (about 1 GPa), 2% hydrogel reduced HOXB4 and PROX1 gene expression (Figure 8D). The 4% hydrogel still maintained a high level of HOXB4 but reduced PROX1 gene expression. Taken together, these results indicate that the hydrogels with higher modulus support the hindbrain fate of hiPSC spheroids.

DISCUSSION

Biomaterials play an important role in promoting cell−cell interactions during neural patterning of brain organoids.[11−13] The accurate control of compartmentation within brain organoids needs the understanding and modulation of the extracellular microenvironment of hiPSC-derived spheroids. ECMs of the brain support the survival, migration, and differentiation of neural progenitors, among which hyaluronic acid is a critical component.[23,56] Therefore, HA is a suitable biomaterial for brain tissue engineering and has been widely used for culturing and transplantation of neural progenitors.[27,36] Modified HA hydrogels can increase cell adhesion and promote neurite sprouting, axonal growth, and cellular integration into the damaged tissue.[26] Studies also have shown that NPCs seeded into HA-based 3D hydrogels survive and mature both *in vitro* and *in vivo*.[24] HA hydrogels with tunable mechanical properties were reported to affect the differentiation of NPCs.[57] Stiffer HA hydrogels lead to more astrocyte differentiation while softer HA hydrogels result in more neuronal differentiation.[58] In our study, a higher modulus of Hep-HA hydrogels promoted more stress fiber

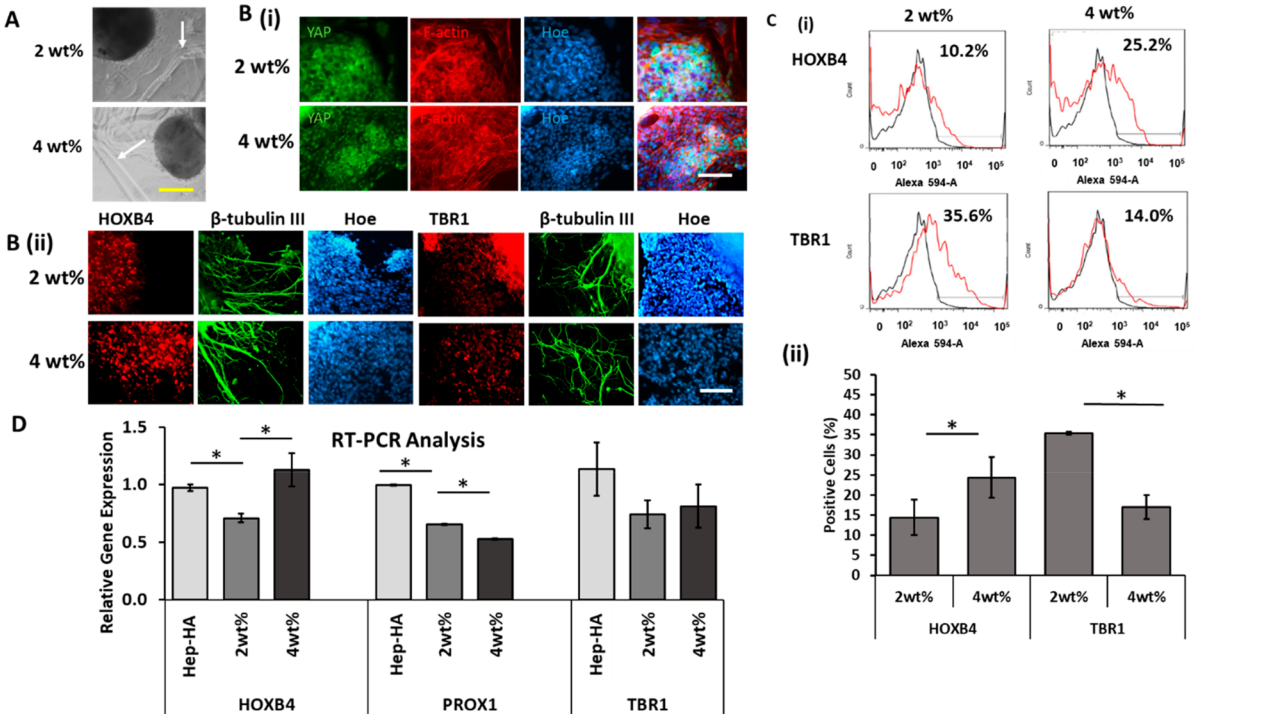

Figure 8. Neural patterning of Hep-HA hydrogels with different moduli. The cells treated with different Hep-HA hydrogels (2 and 4 wt %) at day 16 were analyzed for forebrain and hindbrain markers. (A) Phase contrast images of spheroids within Hep-HA hydrogels; white arrows point to the hydrogel boundary. Scale bar: 200 μm. (B, i) Fluorescent images of forebrain marker TBR1 and hindbrain marker HOXB4 at day 24. (ii) Fluorescent images of YAP and F-actin at day 24. Scale bar: 100 μm. (C) (i) Representative flow cytometry histograms of TBR1 and HOXB4 expression. (ii) Quantification of TBR1 and HOXB4 expression with flow cytometry (n = 3; one-way ANOVA, F-value = 12.06, and P-value = 0.01). (D) RT-PCR analysis of HOXB4, PROX1, and TBR1 gene expression (one-way ANOVA, F-value = 6.02, and P-value = 0.001). * indicates $p < 0.05$.

DOI: 10.1021/acsbiomaterials.8b01142
ACS Biomater. Sci. Eng. 2018, 4, 4354−4366

stretching and more nuclear YAP expression compared to the lower modulus Hep-HA hydrogels. The higher modulus hydrogels also supported the hindbrain fate during hiPSC neural pattening, whereas the lower modulus hydrogel supported forebrain marker expression. However, hydrogel degradability may affect cellular response to the hydrogel stiffness and thus YAP localization, which needs to be investigated further for neural patterning of hiPSCs.

Hydrogels made of pure HA promote cell aggregation, reminiscent of 3D structure.[29] Modified HA hydrogels can promote morphogen-induced differentiation of NPCs into neurons as well as neurite outgrowth and synapse formation compared to traditional 2D cultures.[27] Even though hyaluronan hydrogels induce neurite outgrowth, the cell attachment on HA is low, and binding materials are needed to support cell attachment. Heparin can bind with several growth factors (e.g., BDNF and FGF-2) and has been reported to express various binding abilities with different ECMs.[59] For example, heparin and RGD peptides promoted 25-fold higher neurite outgrowth compared to nonfunctionalized HA hydrogels.[24] Also, it has been reported that hyaluronan−heparin−collagen hydrogels reduced inflammatory reaction and supported cell survival after stroke in rodent models.[60] Heparin-decorated HA hydrogels can also be used for the controlled release of growth factors (e.g., BMP-2) to the cells.[30]

In this study, undifferentiated iPSK3 cells were treated with three types of ECMs (gelatin, hyaluronic acid, Hep-HA). The results indicate that the Hep-HA group favors the ectoderm differentiation of hiPSCs compared to HA alone. The cortical spheroids treated with different ECMs were analyzed for brain region-identity markers. The Hep-HA treatment increases the expression of hindbrain markers HOXB4 and ISL1 compared to HA alone and gelatin. Heparin is reported to be a reservoir of many growth factors (e.g., BDNF and BMP-2), which could impact neural patterning. The cells were also treated with ECMs at an earlier stage of cortical tissue development. The results indicate that Hep-HA effects on the neural patterning depend on development stages (e.g., days 8 and 16). Different biomaterials support the expression of different receptors on the stem cells (through receptor−ligand binding)[61] and were reported to impact various signaling (e.g., Wnt and Hippo) in the cells.[39] This leads to the hypothesis that the impact of these ECMs on neural patterning of hiPSCs might act through cell signaling pathways.

The results of our study reveal that the cells on each type of ECM express distinct stress fiber formation. Since the morphological changes of cells result in the shuttling of cellular mechanosensor YAP,[62,63] the expression of YAP and its localization of cells grown on these ECMs were evaluated. High expression of nuclear YAP was observed in the cells treated with Hep-HA hydrogels, suggesting that heparin may promote nuclear YAP localization. YAP/TAZ localization influences the translocation of β-catenin (e.g., Hep-HA promotes nuclear expression of active β-catenin) and thereby leads to the activation of canonical Wnt signaling.[43,55] Our results indicate that YAP modulation using Cyto D (induces cytoplasmic YAP) inhibits the canonical Wnt signaling elicited by Hep-HA hydrogels. This leads to the necessity of evaluating the impact of heparin on Wnt signaling and the corresponding impact on neural patterning.

In our study, the cells were treated with Wnt inhibitor IWP4 together with the ECMs for evaluating the impact of Wnt signaling on the ECM-patterning effects. The IWP4 treatment abolished the effects of Hep-HA treated cells, indicating that the cells in the Hep-HA group may express elevated Wnt signaling. Previous studies demonstrate the involvement of heparin in different cell signaling pathways including Wnt signaling.[38] For example, heparan sulfate binds with Wnt signals and supports its stability in ECM and also prevents the aggregation of Wnt proteins in aqueous environments.[40] Moreover, heparan sulfates/heparin promote the stability and interaction of the sFRPs, which act as a biphasic modulator of Wnt and the coreceptors that directly facilitate the formation of Wnt-Fz signaling complexes.[41] Since Wnt proteins activate several signaling cascades and support differentiation of stem cells into either cardiac or neural lineage,[38,42] heparin has been used in neural differentiation and maturation of cells through modulating Wnt signaling. For example, heparin can modulate Wnt3a-induced stabilization of β-catenin and supports morphological differentiation of both N2a and hippocampal cells.[39] Heparin incubation also decreased glycogen synthase kinase 3 beta activity in a concentration-dependent manner in N2a cells. Taken together, our Hep-HA hydrogels allow for optimization of ECM stiffness as well as the presentation of biochemical ligands (heparin-binding effects) to regulate neural patterning for brain organoid engineering.[4]

While the Wnt pathway can pattern neural tissues derived from hiPSCs along the rostral and caudal brain identity,[42,43] it also plays a key role in dorsal-ventral patterning.[64] The influence of Wnt and/or Hippo/YAP signaling on dorsal-ventral patterning of hiPSCs remain to be examined in the future. In addition, while this study focuses on the heparin effect on Wnt signaling, potentially, any heparin-binding growth factors (e.g., FGF-2, BDNF) can be linked to the heparin-HA hydrogels to influence neural patterning during organoid formation from hiPSCs. Moreover, hydrogel degradability may affect the cell response to the hydrogel stiffness and thus YAP localization,[65] which needs to be investigated further for neural patterning.

It needs to be noted that large variabilities in spheroid-based cultures pose difficulties in analyzing different cell types.[66] Large variations exist in aggregate size and cell diversity in the aggregates/spheroids. While single aggregate formation methods (e.g., using glow attachment 96-well plate) can reduce the variations, they are not easily handled for experiments on a larger scale. Modification of medium formulation to generate uniform spheroids is desirable.[67]

CONCLUSIONS

This study investigates the synergistic effects of heparin and hyaluronic acid on neural patterning of hiPSC-derived cortical spheroids. Hep-HA favors ectoderm differentiation of hiPSCs. The treatment of cortical spheroids with the Hep-HA at a late stage biases the neural patterning toward a hindbrain fate. The detailed evaluation of the underlying effects of different ECMs reveals that Hep-HA elevates Wnt signaling compared to HA alone. Modulation of the Hippo/Yap signaling also influences the patterning effect of these ECMs. A comparative study with Hep-HA hydrogels with varying modulus reveals that the lower modulus (300−400 Pa) supports the forebrain fate, whereas a higher modulus (1000−1300 Pa) supports the hindbrain fate. Taken together, the Hep-HA hydrogels can interfere with the cell signaling inside the cells and thereby influence neural patterning of hiPSCs.

DOI: 10.1021/acsbiomaterials.8b01142
ACS Biomater. Sci. Eng. 2018, 4, 4354−4366

■ ASSOCIATED CONTENT

Supporting Information

The Supporting Information is available free of charge on the ACS Publications website at DOI: 10.1021/acsbiomaterials.8b01142.

(Figure S1) ^{1}H NMR histogram confirming the methylation of HA; (Figure S2) synthesis of thiolated-heparin (Hep-SH); (Figure S3) pluripotent marker expression for hiPSCs grown with mTeSR + ECM medium; (Figure S4) illustration of the cortical neural spheroid differentiation protocols from hiPSCs; (Figure S5) effect of ECMs on the viability of neural spheroid outgrowth; (Figure S6) effects of ECMs on neural lineage commitment of hiPSCs; (Figure S7) influence of ECM treatment on expression of glutamate and GABA; (Figure S8) effects of ECM treatment on the expression of F-actin stress fiber and outgrowth proliferation; (Figure S9) enlarged confocal images of YAP from the represented groups to show cytoplasmic and nuclear YAP (supporting data for Figure 4Bi); (Figure S10) supporting data (another two repeats) for Western blot of active β-catenin; (Figure S11) active beta-catenin expression under IWP4 treatment; (Figure S12) BRN2 and PROX1 expression for cortical spheroids outgrowth cultured within different Hep-HA hydrogels; (Table S1) list of antibodies; (Table S2) primer sequence for target genes; (Table S3) two-way ANOVA analysis for Figures 3, 5, and 6 (PDF)

■ AUTHOR INFORMATION

Corresponding Author

*Address: 2525 Pottsdamer St., Tallahassee, FL 32310. Tel.: 850-410-6320. Fax: 850-410-6150. E-mail: yli@eng.fsu.edu.

ORCID

Yan Li: 0000-0002-5938-8519

Present Addresses

‖Mailing address for J.B., B.B., T.M., and Y.L.: 2525 Pottsdamer St., A131, Tallahassee, FL 32310, USA.

⊥Mailing address for Z.W., M.Y., and Q.-X.S.: 95 Chieftan Way, Tallahassee, Florida, 32306−4390, USA.

Notes

The authors declare no competing financial interest.

■ ACKNOWLEDGMENTS

The authors would like to thank Ms. Ruth Didier in the FSU Department of Biomedical Sciences for her help with flow cytometry analysis, Dr. Brian K. Washburn and Kristina Poduch in the FSU Department of Biological Sciences for their help with RT-PCR analysis, Dr. Stephen Duncan at the Medical College of Wisconsin, and Dr. David Gilbert in the FSU Department of Biological Sciences for human iPSK3 cells. This work is supported by FSU start-up fund and partially from National Science Foundation (CAREER award, grant no. 1652992 to Y.L.). Research reported in this publication was also supported by the National Institute of Neurological Disorders and Stroke of the National Institutes of Health (USA) under Award Number R03NS102640 (to Y.L.). The content is solely the responsibility of the authors and does not necessarily represent the official views of the National Institutes of Health.

■ REFERENCES

(1) Lancaster, M. A.; Renner, M.; Martin, C. A.; Wenzel, D.; Bicknell, L. S.; Hurles, M. E.; Homfray, T.; Penninger, J. M.; Jackson, A. P.; Knoblich, J. A. Cerebral organoids model human brain development and microcephaly. *Nature* **2013**, *501*, 373−9.

(2) Lancaster, M. A.; Knoblich, J. A. Organogenesis in a dish: modeling development and disease using organoid technologies. *Science* **2014**, *345*, 1247125.

(3) Qian, X.; Nguyen, H. N.; Song, M. M.; Hadiono, C.; Ogden, S. C.; Hammack, C.; Yao, B.; Hamersky, G. R.; Jacob, F.; Zhong, C.; Yoon, K. J.; Jeang, W.; Lin, L.; Li, Y.; Thakor, J.; Berg, D. A.; Zhang, C.; Kang, E.; Chickering, M.; Nauen, D.; Ho, C. Y.; Wen, Z.; Christian, K. M.; Shi, P. Y.; Maher, B. J.; Wu, H.; Jin, P.; Tang, H.; Song, H.; Ming, G. L. Brain-region-specific organoids using mini-bioreactors for modeling ZIKV exposure. *Cell* **2016**, *165*, 1238−1254.

(4) Yin, X.; Mead, B. E.; Safaee, H.; Langer, R.; Karp, J. M.; Levy, O. Engineering stem cell organoids. *Cell Stem Cell* **2016**, *18*, 25−38.

(5) Di Lullo, E.; Kriegstein, A. R. The use of brain organoids to investigate neural development and disease. *Nat. Rev. Neurosci.* **2017**, *18*, 573−584.

(6) Xiang, Y.; Tanaka, Y.; Patterson, B.; Kang, Y. J.; Govindaiah, G.; Roselaar, N.; Cakir, B.; Kim, K. Y.; Lombroso, A. P.; Hwang, S. M.; Zhong, M.; Stanley, E. G.; Elefanty, A. G.; Naegele, J. R.; Lee, S. H.; Weissman, S. M.; Park, I. H. Fusion of Regionally Specified hPSC-Derived Organoids Models Human Brain Development and Interneuron Migration. *Cell Stem Cell* **2017**, *21*, 383−398.

(7) Yan, Y.; Song, L.; Bejoy, J.; Zhao, J.; Kanekiyo, T.; Bu, G.; Zhou, Y.; Li, Y. Modelling neurodegenerative microenvironment using cortical organoids derived from human stem cells. *Tissue Eng., Part A* **2018**, *24*, 1125−1137.

(8) Li, Y.; Xu, C.; Ma, T. In vitro organogenesis from pluripotent stem cells. *Organogenesis* **2014**, *10*, 159−163.

(9) Song, L.; Tsai, A. C.; Yuan, X.; Bejoy, J.; Sart, S.; Ma, T.; Li, Y. Neural differentiation of spheroids derived from human induced pluripotent stem cells-mesenchymal stem cells co-culture. *Tissue Eng., Part A* **2018**, *24*, 915−929.

(10) Jorfi, M.; D'Avanzo, C.; Tanzi, R. E.; Kim, D. Y.; Irimia, D. Human Neurospheroid Arrays for In Vitro Studies of Alzheimer's Disease. *Sci. Rep.* **2018**, *8* (1), 2450.

(11) Marti-Figueroa, C. R.; Ashton, R. S. The case for applying tissue engineering methodologies to instruct human organoid morphogenesis. *Acta Biomater.* **2017**, *54*, 35−44.

(12) Shah, S. B.; Singh, A. Cellular self-assembly and biomaterials-based organoid models of development and diseases. *Acta Biomater.* **2017**, *53*, 29−45.

(13) Wan, A. C. Recapitulating cell-cell interactions for organoid construction - are biomaterials dispensable? *Trends Biotechnol.* **2016**, *34*, 711−721.

(14) Gjorevski, N.; Ranga, A.; Lutolf, M. P. Bioengineering approaches to guide stem cell-based organogenesis. *Development* **2014**, *141*, 1794−804.

(15) Pasca, S. P. The rise of three-dimensional human brain cultures. *Nat. Neurosci.* **2018**, *553*, 437−445.

(16) Oyama, H.; Takahashi, K.; Tanaka, Y.; Takemoto, H.; Haga, H. Long-term Culture of Human iPS Cell-derived Telencephalic Neuron Aggregates on Collagen Gel. *Cell Struct. Funct.* **2018**, *43*, 85−94.

(17) Ranga, A.; Girgin, M.; Meinhardt, A.; Eberle, D.; Caiazzo, M.; Tanaka, E. M.; Lutolf, M. P. Neural tube morphogenesis in synthetic 3D microenvironments. *Proc. Natl. Acad. Sci. U. S. A.* **2016**, *113*, E6831−E6839.

(18) Jorfi, M.; D'Avanzo, C.; Kim, D. Y.; Irimia, D. Three-dimensional models of human brain development and diseases. *Adv. Healthcare Mater.* **2018**, *7*, 1700723.

(19) Madl, C. M.; LeSavage, B. L.; Dewi, R. E.; Dinh, C. B.; Stowers, R. S.; Khariton, M.; Lampe, K. J.; Nguyen, D.; Chaudhuri, O.; Enejder, A.; Heilshorn, S. C. Maintenance of neural progenitor cell stemness in 3D hydrogels requires matrix remodelling. *Nat. Mater.* **2017**, *16*, 1233−1242.

DOI: 10.1021/acsbiomaterials.8b01142
ACS Biomater. Sci. Eng. 2018, 4, 4354−4366

(20) Candiello, J.; Grandhi, T. S. P.; Goh, S. K.; Vaidya, V.; Lemmon-Kishi, M.; Eliato, K. R.; Ros, R.; Kumta, P. N.; Rege, K.; Banerjee, I. 3D heterogeneous islet organoid generation from human embryonic stem cells using a novel engineered hydrogel platform. *Biomaterials* **2018**, *177*, 27−39.
(21) Lindborg, B. A.; Brekke, J. H.; Vegoe, A. L.; Ulrich, C. B.; Haider, K. T.; Subramaniam, S.; Venhuizen, S. L.; Eide, C. R.; Orchard, P. J.; Chen, W.; Wang, Q.; Pelaez, F.; Scott, C. M.; Kokkoli, E.; Keirstead, S. A.; Dutton, J. R.; Tolar, J.; O'Brien, T. D. Rapid Induction of Cerebral Organoids From Human Induced Pluripotent Stem Cells Using a Chemically Defined Hydrogel and Defined Cell Culture Medium. *Stem Cells Transl. Med.* **2016**, *5*, 970−9.
(22) Gong, L.; Cao, L.; Shen, Z.; Shao, L.; Gao, S.; Zhang, C.; Lu, J.; Li, W. Materials for Neural Differentiation, Trans-Differentiation, Modeling of Neurological Disease. *Adv. Mater.* **2018**, *30*, 1705684.
(23) Lau, L. W.; Cua, R.; Keough, M. B.; Haylock-Jacobs, S.; Yong, V. W. Pathophysiology of the brain extracellular matrix: a new target for remyelination. *Nat. Rev. Neurosci.* **2013**, *14*, 722−9.
(24) Adil, M. M.; Vazin, T.; Ananthanarayanan, B.; Rodrigues, G. M. C.; Rao, A. T.; Kulkarni, R. U.; Miller, E. W.; Kumar, S.; Schaffer, D. V. Engineered hydrogels increase the post-transplantation survival of encapsulated hESC-derived midbrain dopaminergic neurons. *Biomaterials* **2017**, *136*, 1−11.
(25) Lam, J.; Lowry, W. E.; Carmichael, S. T.; Segura, T. Delivery of iPS-NPCs to the Stroke Cavity within a Hyaluronic Acid Matrix Promotes the Differentiation of Transplanted Cells. *Adv. Funct. Mater.* **2014**, *24*, 7053−7062.
(26) Highley, C. B.; Prestwich, G. D.; Burdick, J. A. Recent advances in hyaluronic acid hydrogels for biomedical applications. *Curr. Opin. Biotechnol.* **2016**, *40*, 35−40.
(27) Wang, T. W.; Spector, M. Development of hyaluronic acid-based scaffolds for brain tissue engineering. *Acta Biomater.* **2009**, *5*, 2371−84.
(28) Khaing, Z. Z.; Seidlits, S. K. Hyaluronic acid and neural stem cells: implications for biomaterial design. *J. Mater. Chem. B* **2015**, *3*, 7850−7866.
(29) Gerecht, S.; Burdick, J. A.; Ferreira, L. S.; Townsend, S. A.; Langer, R.; Vunjak-Novakovic, G. Hyaluronic acid hydrogel for controlled self-renewal and differentiation of human embryonic stem cells. *Proc. Natl. Acad. Sci. U. S. A.* **2007**, *104*, 11298−303.
(30) Bhakta, G.; Rai, B.; Lim, Z. X.; Hui, J. H.; Stein, G. S.; van Wijnen, A. J.; Nurcombe, V.; Prestwich, G. D.; Cool, S. M. Hyaluronic acid-based hydrogels functionalized with heparin that support controlled release of bioactive BMP-2. *Biomaterials* **2012**, *33*, 6113−22.
(31) Kuo, Y. C.; Hsueh, C. H. Neuronal production from induced pluripotent stem cells in self-assembled collagen-hyaluronic acid-alginate microgel scaffolds with grafted GRGDSP/Ln5-P4. *Mater. Sci. Eng., C* **2017**, *76*, 760−774.
(32) Wu, S.; Xu, R.; Duan, B.; Jiang, P. Three-Dimensional Hyaluronic Acid Hydrogel-Based Models for In Vitro Human iPSC-Derived NPC Culture and Differentiation. *J. Mater. Chem. B* **2017**, *5* (21), 3870−3878.
(33) Arulmoli, J.; Wright, H. J.; Phan, D. T. T.; Sheth, U.; Que, R. A.; Botten, G. A.; Keating, M.; Botvinick, E. L.; Pathak, M. M.; Zarembinski, T. I.; Yanni, D. S.; Razorenova, O. V.; Hughes, C. C. W.; Flanagan, L. A. Combination scaffolds of salmon fibrin, hyaluronic acid, and laminin for human neural stem cell and vascular tissue engineering. *Acta Biomater.* **2016**, *43*, 122−138.
(34) Ekerdt, B. L.; Fuentes, C. M.; Lei, Y.; Adil, M. M.; Ramasubramanian, A.; Segalman, R. A.; Schaffer, D. V. Thermoreversible Hyaluronic Acid-PNIPAAm Hydrogel Systems for 3D Stem Cell Culture. *Adv. Healthcare Mater.* **2018**, *7*, 1800225.
(35) Yu, C.; Griffiths, L. R.; Haupt, L. M. Exploiting Heparan Sulfate Proteoglycans in Human Neurogenesis-Controlling Lineage Specification and Fate. *Front. Integr. Neurosci.* **2017**, *11*, 28.
(36) Bejoy, J.; Song, L.; Wang, Z.; Sang, Q. X.; Zhou, Y.; Li, Y. Neuroprotective Activities of Heparin, Heparinase III, and Hyaluronic Acid on the Aβ42-treated Forebrain Spheroids Derived from Human Stem Cells. *ACS Biomater. Sci. Eng.* **2018**, *4*, 2922−2933.
(37) Roam, J. L.; Nguyen, P. K.; Elbert, D. L. Controlled release and gradient formation of human glial-cell derived neurotrophic factor from heparinated poly(ethylene glycol) microsphere-based scaffolds. *Biomaterials* **2014**, *35*, 6473−81.
(38) Lin, Y.; Linask, K. L.; Mallon, B.; Johnson, K.; Klein, M.; Beers, J.; Xie, W.; Du, Y.; Liu, C.; Lai, Y.; Zou, J.; Haigney, M.; Yang, H.; Rao, M.; Chen, G. Heparin Promotes Cardiac Differentiation of Human Pluripotent Stem Cells in Chemically Defined Albumin-Free Medium, Enabling Consistent Manufacture of Cardiomyocytes. *Stem Cells Transl. Med.* **2017**, *6*, 527−538.
(39) Colombres, M.; Henriquez, J. P.; Reig, G. F.; Scheu, J.; Calderon, R.; Alvarez, A.; Brandan, E.; Inestrosa, N. C. Heparin activates Wnt signaling for neuronal morphogenesis. *J. Cell. Physiol.* **2008**, *216*, 805−15.
(40) Fuerer, C.; Habib, S. J.; Nusse, R. A study on the interactions between heparan sulfate proteoglycans and Wnt proteins. *Dev. Dyn.* **2010**, *239*, 184−190.
(41) Zhong, X.; Desilva, T.; Lin, L.; Bodine, P.; Bhat, R. A.; Presman, E.; Pocas, J.; Stahl, M.; Kriz, R. Regulation of secreted Frizzled-related protein-1 by heparin. *J. Biol. Chem.* **2007**, *282*, 20523−33.
(42) Moya, N.; Cutts, J.; Gaasterland, T.; Willert, K.; Brafman, D. A. Endogenous WNT signaling regulates hPSC-derived neural progenitor cell heterogeneity and specifies their regional identity. *Stem Cell Rep.* **2014**, *3*, 1015−1028.
(43) Bejoy, J.; Song, L.; Zhou, Y.; Li, Y. Wnt-Yes associated protein interactions during neural tissue patterning of human induced pluripotent stem cells. *Tissue Eng., Part A* **2018**, *24*, 546−558.
(44) Si-Tayeb, K.; Noto, F. K.; Sepac, A.; Sedlic, F.; Bosnjak, Z. J.; Lough, J. W.; Duncan, S. A. Generation of human induced pluripotent stem cells by simple transient transfection of plasmid DNA encoding reprogramming factors. *BMC Dev. Biol.* **2010**, *10*, 81.
(45) Si-Tayeb, K.; Noto, F. K.; Nagaoka, M.; Li, J.; Battle, M. A.; Duris, C.; North, P. E.; Dalton, S.; Duncan, S. A. Highly efficient generation of human hepatocyte-like cells from induced pluripotent stem cells. *Hepatology* **2010**, *51*, 297−305.
(46) Yan, Y.; Martin, L.; Bosco, D.; Bundy, J.; Nowakowski, R.; Sang, Q. X.; Li, Y. Differential effects of acellular embryonic matrices on pluripotent stem cell expansion and neural differentiation. *Biomaterials* **2015**, *73*, 231−242.
(47) Song, L.; Wang, K.; Li, Y.; Yang, Y. Nanotopography promoted neuronal differentiation of human induced pluripotent stem cells. *Colloids Surf., B* **2016**, *148*, 49−58.
(48) Gwon, K.; Kim, E.; Tae, G. Heparin-hyaluronic acid hydrogel in support of cellular activities of 3D encapsulated adipose derived stem cells. *Acta Biomater.* **2017**, *49*, 284−295.
(49) Tae, G.; Kim, Y. J.; Choi, W. I.; Kim, M.; Stayton, P. S.; Hoffman, A. S. Formation of a novel heparin-based hydrogel in the presence of heparin-binding biomolecules. *Biomacromolecules* **2007**, *8*, 1979−86.
(50) Yan, Y.; Bejoy, J.; Xia, J.; Guan, J.; Zhou, Y.; Li, Y. Neural patterning of human induced pluripotent stem cells in 3-D cultures for studying biomolecule-directed differential cellular responses. *Acta Biomater.* **2016**, *42*, 114−126.
(51) Yan, Y.; Song, L.; Madinya, J.; Ma, T.; Li, Y. Derivation of cortical spheroids from human induced pluripotent stem cells in a suspension bioreactor. *Tissue Eng., Part A* **2018**, *24*, 418−431.
(52) Sart, S.; Yan, Y.; Li, Y.; Lochner, E.; Zeng, C.; Ma, T.; Li, Y. Crosslinking of extracellular matrix scaffolds derived from pluripotent stem cell aggregates modulates neural differentiation. *Acta Biomater.* **2016**, *30*, 222−232.
(53) Sart, S.; Ma, T.; Li, Y. Extracellular matrices decellularized from embryonic stem cells maintained their structure and signaling specificity. *Tissue Eng., Part A* **2014**, *20*, 54−66.
(54) Xu, Y.; Stamenkovic, I.; Yu, Q. CD44 attenuates activation of the hippo signaling pathway and is a prime therapeutic target for glioblastoma. *Cancer Res.* **2010**, *70*, 2455−64.

DOI: 10.1021/acsbiomaterials.8b01142
ACS Biomater. Sci. Eng. 2018, 4, 4354−4366

(55) Azzolin, L.; Panciera, T.; Soligo, S.; Enzo, E.; Bicciato, S.; Dupont, S.; Bresolin, S.; Frasson, C.; Basso, G.; Guzzardo, V.; Fassina, A.; Cordenonsi, M.; Piccolo, S. YAP/TAZ incorporation in the beta-catenin destruction complex orchestrates the Wnt response. *Cell* **2014**, *158*, 157−70.
(56) Fowke, T. M.; Karunasinghe, R. N.; Bai, J. Z.; Jordan, S.; Gunn, A. J.; Dean, J. M. Hyaluronan synthesis by developing cortical neurons in vitro. *Sci. Rep.* **2017**, *7*, 44135.
(57) Seidlits, S. K.; Khaing, Z. Z.; Petersen, R. R.; Nickels, J. D.; Vanscoy, J. E.; Shear, J. B.; Schmidt, C. E. The effects of hyaluronic acid hydrogels with tunable mechanical properties on neural progenitor cell differentiation. *Biomaterials* **2010**, *31*, 3930−40.
(58) Liu, Z.; Tang, M.; Zhao, J.; Chai, R.; Kang, J. Looking into the Future: Toward Advanced 3D Biomaterials for Stem-Cell-Based Regenerative Medicine. *Adv. Mater.* **2018**, *30*, 1705388.
(59) Benoit, D. S.; Anseth, K. S. Heparin functionalized PEG gels that modulate protein adsorption for hMSC adhesion and differentiation. *Acta Biomater.* **2005**, *1*, 461−70.
(60) Zhong, J.; Chan, A.; Morad, L.; Kornblum, H. I.; Fan, G.; Carmichael, S. T. Hydrogel matrix to support stem cell survival after brain transplantation in stroke. *Neurorehabil Neural Repair* **2010**, *24*, 636−44.
(61) Guilak, F.; Cohen, D. M.; Estes, B. T.; Gimble, J. M.; Liedtke, W.; Chen, C. S. Control of stem cell fate by physical interactions with the extracellular matrix. *Cell Stem Cell* **2009**, *5*, 17−26.
(62) Konsavage, W. M., Jr.; Yochum, G. S. Intersection of Hippo/YAP and Wnt/beta-catenin signaling pathways. *Acta Biochim. Biophys. Sin.* **2013**, *45*, 71−9.
(63) Sun, Y.; Yong, K. M.; Villa-Diaz, L. G.; Zhang, X.; Chen, W.; Philson, R.; Weng, S.; Xu, H.; Krebsbach, P. H.; Fu, J. Hippo/YAP-mediated rigidity-dependent motor neuron differentiation of human pluripotent stem cells. *Nat. Mater.* **2014**, *13*, 599−604.
(64) Muguruma, K. Self-Organized Cerebellar Tissue from Human Pluripotent Stem Cells and Disease Modeling with Patient-Derived iPSCs. *Cerebellum* **2018**, *17*, 37−41.
(65) Caliari, S. R.; Vega, S. L.; Kwon, M.; Soulas, E. M.; Burdick, J. A. Dimensionality and spreading influence MSC YAP/TAZ signaling in hydrogel environments. *Biomaterials* **2016**, *103*, 314−323.
(66) Quadrato, G.; Nguyen, T.; Macosko, E. Z.; Sherwood, J. L.; Min Yang, S.; Berger, D. R.; Maria, N.; Scholvin, J.; Goldman, M.; Kinney, J. P.; Boyden, E. S.; Lichtman, J. W.; Williams, Z. M.; McCarroll, S. A.; Arlotta, P. Cell diversity and network dynamics in photosensitive human brain organoids. *Nature* **2017**, *545*, 48−53.
(67) Lipsitz, Y. Y.; Tonge, P. D.; Zandstra, P. W. Chemically controlled aggregation of pluripotent stem cells. *Biotechnol. Bioeng.* **2018**, *115*, 2061−2066.

DOI: 10.1021/acsbiomaterials.8b01142
ACS Biomater. Sci. Eng. 2018, 4, 4354−4366